Paleomagnetism of DSDP Sediments, Phase Shifting of Magnetic Anomalies, and Rotations of the West Philippine Basin

KEITH E. LOUDEN[1]

MIT/Woods Hole Oceanographic Institution Joint Program in Oceanography
Department of Earth and Planetary Sciences, Massachusetts Institute of Technology, Cambridge, Massachusetts 02138

A paleomagnetic study of sediments from Deep-Sea Drilling Project (DSDP) sites 290, 292, and 294 suggests that the West Philippine Basin originated between 5° and 10°S. Results for site 292 are particularly consistent; a group of 20 closely spaced samples at the sediment-basalt interface has a mean absolute paleolatitude and 95% confidence interval of 4.9° ± 2.0°. An equatorial crossing is implied by the trend of paleoinclinations as a function of age for 73 additional samples from site 292 and concurrent results from sites 290 and 294. Origin of the West Philippine Basin in southern latitudes is also consistent with the phase shifting of marine magnetic anomalies, which must be inverted to be matched with a set of worldwide Eocene reversals. Two well-defined paleomagnetic pole positions are determined if the low amplitude of these east-west anomalies, in comparison to similarly oriented anomalies in the Pacific and Indian oceans, is due to a rotation of this plate. One of these is consistent with paleopoles calculated from the 'absolute' motion of the Pacific and directions of relative motion between the Philippine and the Pacific plate. This suggests a clockwise rotation of 60° between the Philippine plate and the magnetic pole and is similar to results from the study of Miocene rocks on Guam. This may imply that both Guam and the West Philippine Basin have undergone the same past plate motion and that the rotation of Guam is not due to a simple bending of the Marianas arc.

INTRODUCTION

There are essentially four methods by which we can determine the rotations of the plates relative to an external frame of reference. These are (1) the paleomagnetic study of basalts and sediments, (2) the phase or shape analysis of linear sea floor spreading and seamount magnetic anomalies, (3) the bathymetric mapping of hot spot traces, and (4) the location of deepwater regions of high sedimentation, which are assumed to be produced within ±5° of the paleoequator. If it is then assumed that the earth's paleomagnetic field has time-averaged over 10^4–10^5 years to an axially geocentric dipole concordant with the spin axis [*Opdyke*, 1972] and that hot spots have remained fixed with respect to this axis, then all of these measurements are directly comparable. Such 'absolute' motions have been determined in this manner for the South Atlantic [*Phillips and Forsyth*, 1972; *Lowrie et al.*, 1973*b*], North Pacific [*Francheteau et al.*, 1970; *Clague and Jarrard*, 1973; *Harrison et al.*, 1975], and Indian [*McKenzie and Sclater*, 1971; *Blow and Hamilton*, 1975] oceans, and results based on the different techniques are generally consistent [*Peirce*, 1976]. These studies have been particularly successful in recording the northward motion of the Pacific and Indian plates since the Cretaceous.

This paper attempts to use some of the same techniques in placing constraints on the early history and subsequent motion of the Philippine plate. A comparison of the absolute motions of the Pacific and Philippine plates can hopefully lead to some understanding of how these two plates have moved in relation to each other. This is important, since the nature of relative motions produced by inner arc spreading is not well understood. Determinations of instantaneous motion are based almost entirely on fault plane solutions [*Katsumata and Sykes*, 1969; *Fitch*, 1972], and the results are only poorly constrained, as is evidenced by the many different locations of possible Philippine-Pacific poles [*Karig*, 1975].

Almost nothing certain is known about motions of the Philippine plate over a finite length of time. The primary reason for this is the absence of easily identifiable magnetic anomalies in both active (young) and inactive (old) basins of the Philippine Sea. Recently, however, *Louden* [1976] has identified some anomalies in the West Philippine Basin across the Central Basin Fault (Figures 1 and 10). This region is one of the older sections of the Philippine Sea, but controversy still exists over its exact age and origin. One theory forms the West Philippine Basin by inner arc spreading during an Eocene pulse similar to but in a different direction from that which later opened the more eastern Parece Vela and Shikoku basins [*Karig*, 1975]. Another explains it as a remanent of the Mesozoic Kula-Pacific ridge system which was trapped when the absolute motion of the Pacific changed direction 40 m.y. ago [*Uyeda and Ben-Avraham*, 1972]. This theory is inconsistent with ages based on Joides cores, magnetic anomaly identifications, and heat flow averages, which all indicate an Eocene age [*Louden*, 1976]. Only the 6-km depth of the basin, which gives a minimum age of 80 m.y. from the depth versus age curves of the Pacific [*Sclater et al.*, 1971], is consistent with this interpretation, but it is not certain whether depth versus age curves for major ocean basins can be applied to marginal basins [*Sclater et al.*, 1976].

Initial analysis of the skewness of the magnetic anomalies indicated that they must have been formed 0°–16° south of the equator. The total amount of northward motion is very similar to that of the Pacific plate over the same time period (40–50 m.y.). In this paper we will add to these results a study of paleolatitudes derived from sediments taken at three DSDP sites (290, 292, and 294). We also have reanalyzed the magnetic anomalies by using a slightly larger data set. These two analyses (phase shifting and paleomagnetics) can be combined to determine geomagnetic pole positions well constrained in latitude but not in longitude. In addition, the low amplitudes of our magnetic anomalies suggest that they must have undergone significant declinational change since they were formed if their origins are similar to those of anomalies in other ocean basins. One of the two possible pole positions, which is con-

[1]Now at Department of Geodesy and Geophysics, Cambridge University, Cambridge CB3 OEZ, England.

Paper number 7B0211.

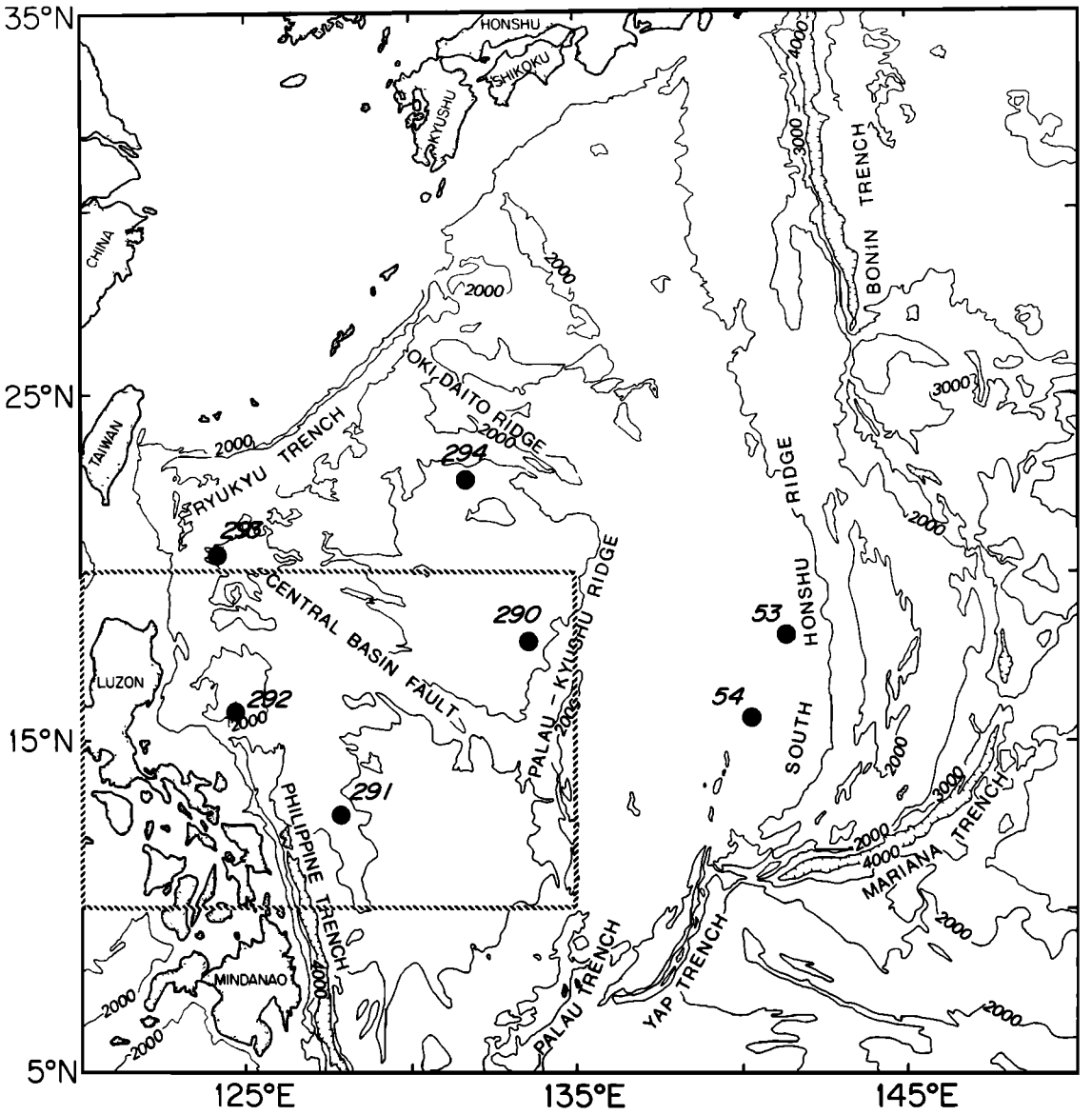

Fig. 1. Bathymetric map of the Philippine Sea from *Chase and Menard* [1969] with uncorrected 1829-m (1000-fathom) contours and selected DSDP site locations. The dashed line encloses the area of Figure 10.

sistent with these magnetic anomaly phase and amplitude criteria and the paleomagnetic inclinations, would require significant rotations (80°–100°) about a relative Pacific-Philippine pole similar to those determined from present-day motions. Paleomagnetic results for basalts from Guam [*E. E. Larson et al.*, 1975] can also be explained by the same 'polar wandering' curve.

Paleomagnetism of DSDP Sediments

Introduction

The paleomagnetic study of deep-sea sediment cores has led to significant advances both in our knowledge of the magnetic reversal stratigraphy over the last 20 m.y. and in understanding the nature of secular variation and excursions in the earth's magnetic field of much shorter duration [*Opdyke*, 1972; *Harrison*, 1974; *Creer et al.*, 1972]. The major advantage of sediments is that unlike the basalts they can offer a semicontinuous record of the magnetic field direction and intensity. The detail of such a record depends directly upon the rate of sedimentation. Low rates (0.1 cm/10^3 yr) will average out most of the secular variation in a standard sample 2.54 cm thick, whereas samples with high sedimentation rates (10 cm/10^3 yr) can record the details of variations over several hundred years.

Successful studies of the sediment paleomagnetic record are possible even though relatively little is known about the mechanisms by which the magnetic pattern is recorded. The slow deposition of sediment grains on the ocean floor (detrital remanent magnetization), postdepositional mixing such as is caused by bioturbation (postdetrital remanent magnetization), and chemical alteration (chemical remanent magnetization) may all play a role. Measurements on many cores of differing lithologies show that some offer coherent patterns in agreement with results from land basalts and sea floor spreading anomalies, while others are scattered with unrecognizable patterns. We do not understand why this happens. Our confidence in the reliability of any particular sediment record is based more on macroscopic properties, such as the statistics of

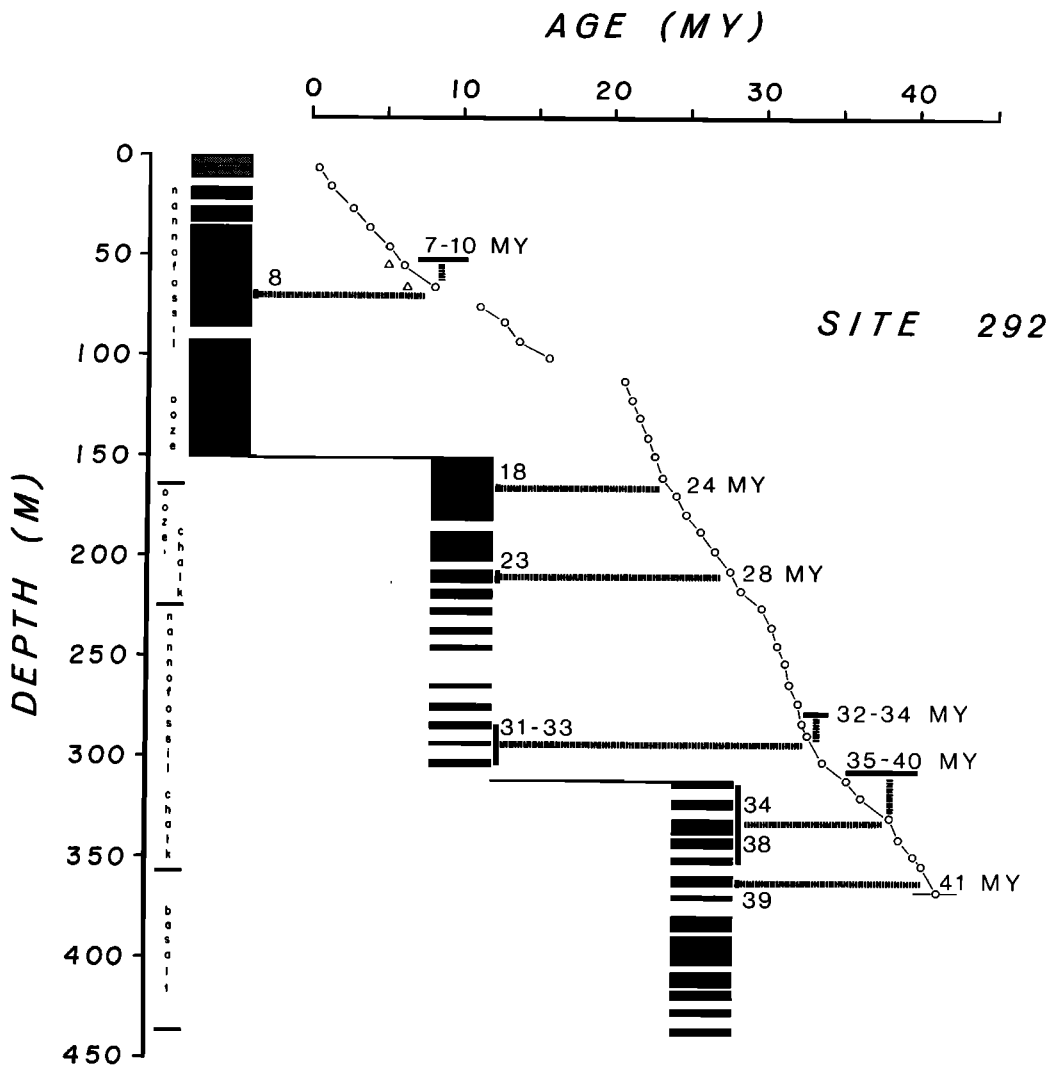

Fig. 2. Lithological and paleontological stratigraphy for DSDP site 292 sediment from *Ingle et al.* [1975] using the *Berggren* [1972] Cenozoic time scale. Shaded areas locate positions of recovered sediment. Numbers identify the location and age of cores which were densely sampled. Paleomagnetic measurements were made on 10–20 10-cm^3 samples as closely spaced as possible in each of these six locations for a total of 93 individual samples.

the scatter in inclination and declination directions, than on any fundamental paleomagnetic properties of the minerals which carry the signal. This poses a significant problem for the analysis of DSDP cores. Because of probable rotations during the drilling process, declination values are always highly scattered, and reversal chronologies can only be determined by changes in sign of the inclination, which may be unreliable for low latitudes. Results often have not been easy to interpret, and attempts at utilizing these cores to extend the sequence of reversals back through the Tertiary have made only slow progress.

Recently, there have been attempts at using the Joides data for mapping changes in paleolatitudes back in time [*Sclater and Cox*, 1970; *Hammond et al.*, 1975; *Peirce*, 1976]. Results can become particularly useful when averages are taken of many closely spaced samples, the standard deviation of the mean forming one measure of our confidence in the result [*Green and Brecher*, 1974]. Collections of high-density sampling can be taken at several locations downcore to give averages of paleolatitudes as a function of age. With such a relationship we can hope to distinguish between origins north and south of the equator even if we do not know whether the field was normal or reversed at the time of formation. A pattern of steep to shallow to steep inclinations should define an equatorial crossing even though the polarities of the inclination averages alone are not significant. Such a pattern has been observed in equatorial Pacific piston cores by *Hammond et al.* [1974]. We only must assume that the plate motion is continuous and that abrupt reversals in its direction do not occur.

Site 292

Drill cores from site 292 contain the most complete sediment section to basement of any of the Joides holes in the West Philippine Basin. The lithology of this sediment is a uniform calcareous ooze/chalk rich in nannofossils, indicating that the bottom (now at 2943 m) has remained above the carbonate compensation depth (CCD) throughout its history [*Ingle et al.*, 1975]. Sedimentation rates as determined by these fossils are fairly uniform at approximately 1.0 cm/10^3 yr. Absolute ages can be determined to within several million years from the nannofossil record [*Ellis*, 1975] and *Berggren* [1972] Cenozoic time scale. Levels of bulk magnetization (0.3–4.0 $\times$ 10^{-4}

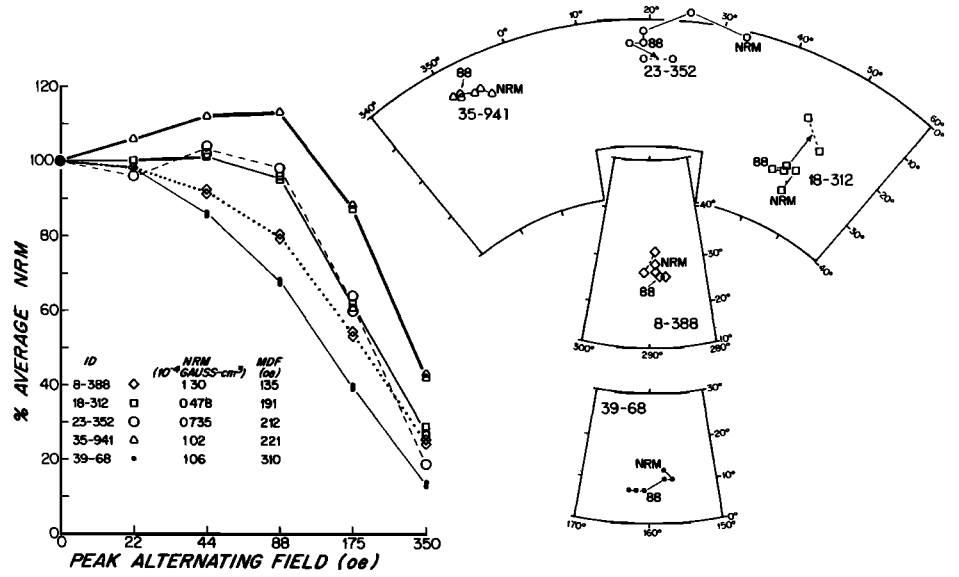

Fig. 3. Demagnetization curves and stereonet plots for selected site 292 sediment intensities and directions. High MDF values and well-grouped directions indicate stable remanent magnetizations.

G cm³) are relatively high because of the large ash content, which probably owes its origins to nearby island arc volcanos. All of these factors plus the undisturbed nature of many of the cores make this a most promising site for paleomagnetic study.

We selected six relatively undisturbed areas at different locations downcore for detailed sampling. These positions together with their associated paleontological ages are shown in Figure 2. At each position we took a suite of 10–20 samples of approximately 10 cm³ each. If the sediment was sufficiently indurated, as it was in cores 31–33, 34–38, and 39, we could sample by diamond drilling, just as we did for the basalts; if not, we took an oriented sample by pressing a nonmagnetic plastic tube (approximately 2.5 × 2.5 cm) into the core by means of a small piston apparatus. The ends of the tube were sealed by epoxy to avoid later disturbances. A total of 94 samples were taken by these techniques and later studied with the use of C. E. Helsley's cryogenic magnetometer and 400-Hz demagnetizer at the University of Texas at Dallas.

We selected five of our samples for detailed af demagnetization experiments, results of which can be seen in Figure 3. The loss of intensity with increasing demagnetization that they show is much less variable from sample to sample than are the changes in direction of magnetization. Some directions vary little from natural remanent magnetization (NRM) to fields of 200 Oe, while others have large variations. *Symons and Stupavsky* [1974] have defined a stability index, PSI, which is

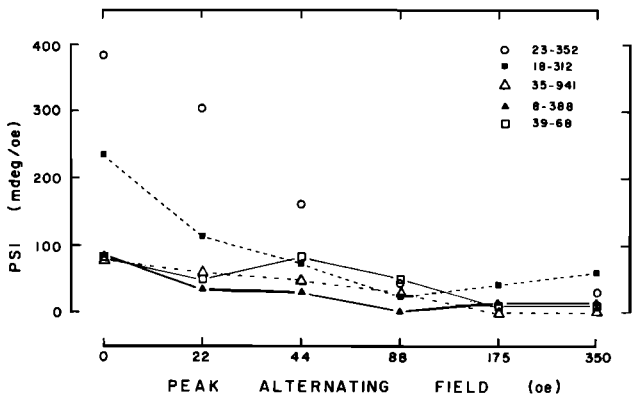

Fig. 4. PSI stability index as a function of demagnetizing field for the same selected site 292 sediments as are shown in Figure 3. Low values at 88–175 Oe indicate moderate to high stability.

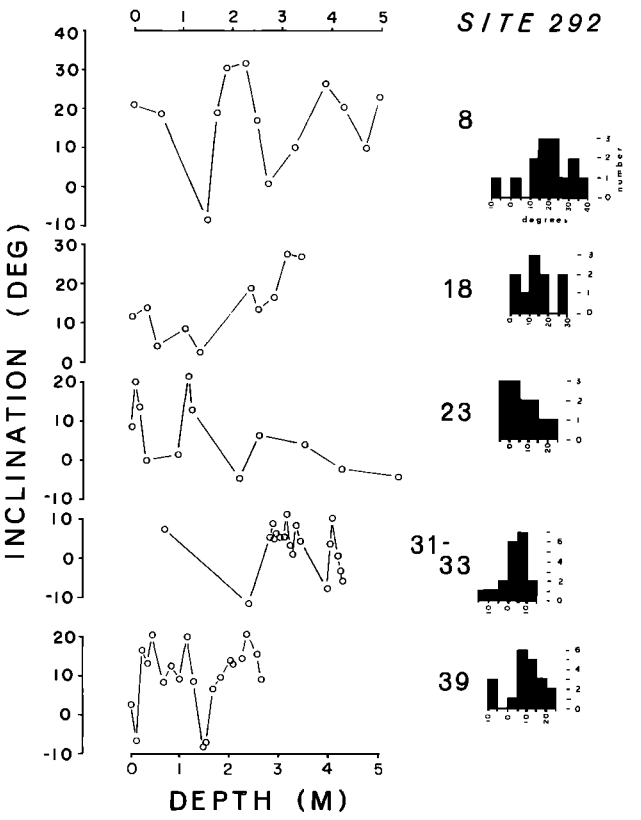

Fig. 5. Paleoinclinations after demagnetization in 88 Oe for site 292 sediments. Large numbers identify the sampling location (see Figure 2) for each group of closely spaced samples. The depth is relative to the position of the top sample in each group. Histograms show the decrease in inclination from cores 8 to 33 and the increase from cores 33 to 39, which we attribute to a crossing of the paleomagnetic equator.

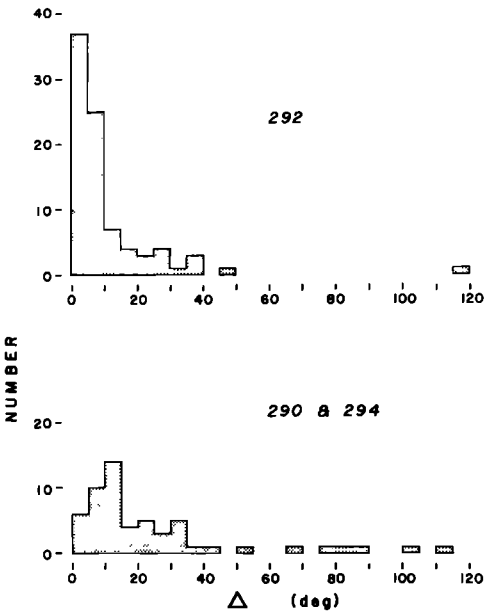

Fig. 6. Histograms of Δ (defined in the text) for sediments of site 292, 290, and 294. Higher values for sites 290 and 294 may indicate greater instability in remanent magnetizations than that for site 292. This is also evidenced by the larger standard errors in mean paleolatitude determinations for sites 290 and 294 (Figure 9) than for site 292 (Figure 7).

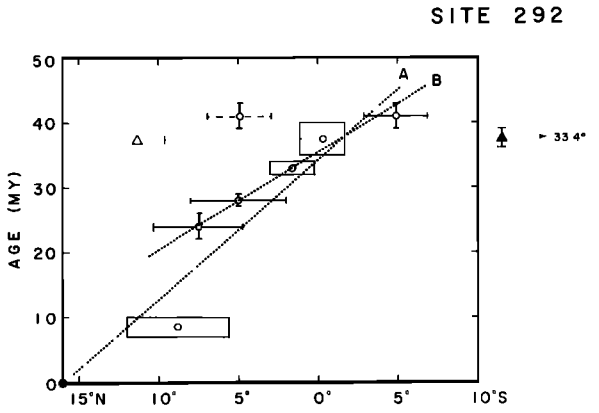

Fig. 7. Age versus mean paleolatitudes for site 292 sediment (circles) and basalt (triangles). Error bars represent ±2 standard errors and include deviations due to theoretical secular variation. Ages are determined from nannofossils [*Ellis*, 1975] and the *Berggren* [1972] Cenozoic time scale. Each mean paleolatitude could be plotted on either side of the equator as is indicated by the two locations for the basalt and the oldest sediment (core 39), but a southern origin is suggested if plate motion is to be uniform. Line A is a visual best fit constrained to go through the present latitude of site 292 (solid circle), while line B fits only the five oldest sediment values. The large range in basalt paleolatitudes is due to insufficient sampling of secular variation and shows that in the absence of multiple basalt flows the sediment data are much more conclusive.

particularly useful when the variation in magnetization direction is of greatest interest. The PSI is a measure of the angular change (in millidegrees) per oersted increase in demagnetizing field; the lower this value is, the more stable the remanence. PSI values are shown in Figure 4 and indicate moderate to high stability at a demagnetization field of 88 Oe. Median destructive fields (MDF) range from 135 to 310 Oe.

On the basis of these results we demagnetized all samples at 88 Oe (see Table 1 for a listing of all our paleomagnetic measurements). Figure 5 is a graph that shows all the demagnetized inclinations in five of our six groups of samples. Values for cores 34–38 were omitted because they span a depth range much greater than that of the others. Histograms of inclinations in each group show a marked decrease from core 8 to 33, followed by an increase from core 33 to 39. This is

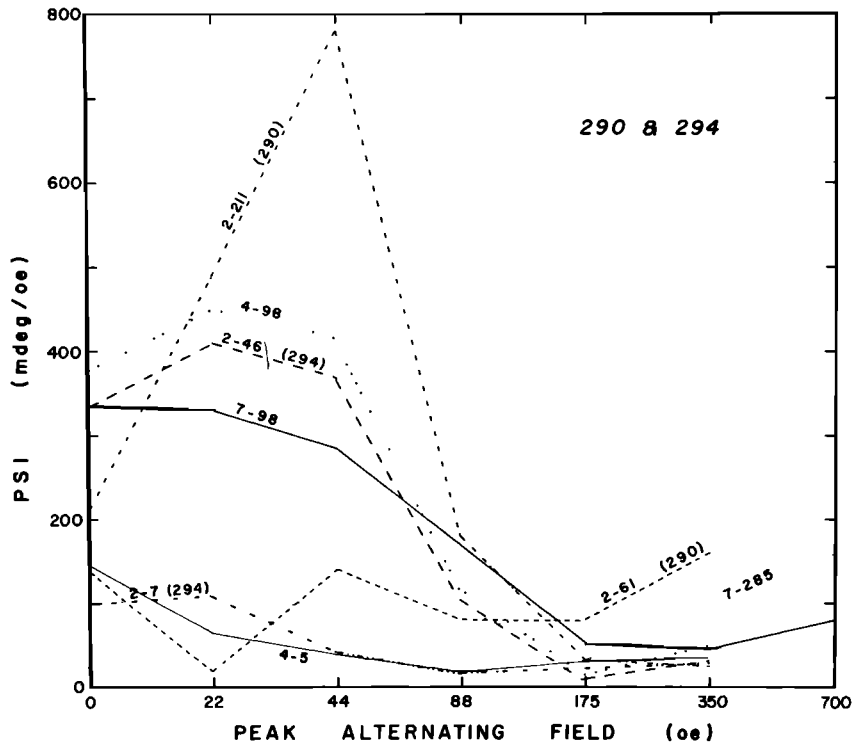

Fig. 8. PSI versus field of demagnetization for selected site 290 and 294 sediments. Lowest values at 175 Oe indicate only moderate to low stability.

TABLE 1. Remanent Magnetic Properties for DSDP Site 292 Sediments

Depth, cm	M_0, 10^{-4} G cm^3	M_{88}, 10^{-4} G cm^3	I_0, deg	I_{88}, deg	D_0, deg	D_{88}, deg	Δ, deg	λ_{88}, deg
			Core 8, N = 13, 66.67 m Below Sea Floor, 7–10 m.y. B.P.					
0	0.518	0.486	22.3	21.1	25.4	23.5	2	10.9
53	1.06	0.821	21.0	18.8	269.7	280.4	10	9.7
152	0.652	0.607	−9.7	−8.6	352.8	354.0	2	−4.3
170	1.04	0.735	19.5	19.0	186.1	185.8	1	9.8
187	0.629	0.531	28.7	30.4	90.1	83.7	6	16.4
226	1.20	0.978	30.1	31.7	119.5	117.0	3	17.2
251	1.43	1.18	17.0	17.1	290.7	297.7	7	8.7
273	0.996	0.768	1.8	0.7	227.8	232.2	5	0.4
291	0.332	0.244	−26.9	(−36.5)	209.3	254.3	39	(−20.3)
328	0.469	0.348	11.4	9.8	245.7	255.5	10	4.9
388	1.30	1.04	27.0	26.4	109.0	106.7	2	13.9
424	1.37	1.13	17.9	20.4	78.2	77.6	3	10.5
470	1.29	1.10	9.5	9.8	335.9	338.5	3	4.9
496	1.05	0.820	21.7	23.0	116.8	115.9	2	12.0
Mean								8.8 (6.8)
σ								5.9 (9.4)
$\sigma/N^{1/2}$								1.6 (2.5)
			Core 18, N = 14, 163.35 m Below Sea Floor, 24 m.y. B.P.					
0	1.00	0.876	14.8	11.7	128.0	133.1	6	5.9
30	1.55	1.14	16.2	13.9	157.4	161.8	5	7.1
58	0.842	0.789	9.8	4.2	213.1	213.2	6	2.1
109	0.564	0.427	−9.6	−8.6	199.1	191.1	8	−4.3
138	0.265	0.225	4.8	−2.3	161.4	135.9	26	−1.2
176	0.102	0.104	0.5	(−2.0)	327.4	212.9	115	(−1.0)
191	0.244	0.139	48.6	(67.8)	210.6	166.1	29	(50.8)
209	0.078	0.124	20.1	(−7.5)	217.4	240.3	36	(−3.8)
222	0.192	0.119	−31.7	(−53.4)	169.2	110.9	47	(−34.0)
241	0.313	0.261	−21.3	−18.8	175.9	164.0	12	−9.7
256	1.30	1.14	−15.5	−13.4	172.7	172.9	2	−6.8
288	0.657	0.715	−11.9	−16.6	213.2	206.9	8	−8.5
312	0.480	0.461	−30.4	−27.7	225.6	222.6	4	−14.7
342	0.612	0.644	−18.8	−26.9	263.9	245.1	19	−14.2
Mean								−7.4 (−4.5)
σ								4.3 (17.3)
$\sigma/N^{1/2}$								1.4 (4.6)
			Core 23, N = 14, 206.03 m Below Sea Floor, 28 m.y. B.P.					
0	0.832	0.513	4.7	−8.8	340.4	324.4	21	−4.4
6	0.627	0.701	−16.4	−19.9	297.6	313.9	16	−10.3
18	0.638	0.500	3.7	−13.7	307.3	277.7	34	−7.0
31	0.893	0.884	−5.1	0.0	79.2	69.3	11	0.0
95	1.70	1.51	0.1	−1.5	186.3	184.3	3	−0.8
115	0.621	0.636	−18.7	−21.7	55.9	77.7	21	−11.3
125	1.30	1.16	−8.7	−13.1	147.3	138.7	10	−6.6
219	0.552	0.654	−8.2	4.4	72.8	60.5	18	2.2
261	1.07	1.24	−4.7	−6.6	349.5	347.0	3	−3.3
282	0.762	0.735	−19.3	(−27.4)	116.5	95.3	21	−14.5
352	0.733	0.722	0.8	−4.2	212.0	198.6	14	−2.1
426	0.749	0.727	3.1	2.2	290.9	295.3	5	1.1
471	1.21	1.04	−25.8	(−28.5)	172.9	173.3	3	−15.2
539	0.422	0.379	22.1	4.2	61.3	81.1	26	2.1
Mean								−5.0
σ								5.7
$\sigma/N^{1/2}$								1.5
			Cores 31–33, N = 19, 283.69 m Below Sea Floor, 32–34 m.y. B.P.					
0	0.683	0.738	7.1	(−21.6)	322.4	321.6	29	(−11.2)
70	0.850	0.819	−8.0	−7.7	263.7	265.1	1	−3.9
154	0.334	0.347	−30.3	(−34.8)	33.4	35.5	5	(−19.2)
241	1.27		11.1		52.7			5.6*
283	1.63	1.57	−5.4	−5.3	4.7	3.4	1	−2.7
288	1.57	1.50	−9.2	−9.0	14.2	12.7	2	−4.5
292	0.875	0.854	−2.2	−4.8	166.1	164.8	3	−2.4
297	0.905	0.877	−6.8	−6.7	160.0	160.4	0	−3.4
302	0.783	0.770	−4.9	−5.5	159.8	158.8	1	−2.8
311	0.714	0.701	−2.3	−5.4	170.8	169.2	4	−2.7
317	0.836	0.832	−12.8	−12.4	261.5	260.8	1	−6.3
323	0.695	0.686	−4.9	−3.4	269.9	269.3	2	−1.7
328	0.559	0.537	−0.8	−1.0	37.8	36.3	2	−0.5
334	0.455	0.445	−8.4	−8.3	40.3	41.3	1	−4.2
343	1.14	1.17	−1.8	−4.3	129.9	131.2	3	−2.2

TABLE 1. (continued)

Depth, cm	M_0, 10^{-4} G cm^3	M_{88}, 10^{-4} G cm^3	I_0, deg	I_{88}, deg	D_0, deg	D_{88}, deg	Δ, deg	λ_{88}, deg
Cores 31–33, N = 19, 283.69 m Below Sea Floor, 32–34 m.y. B.P. (continued)								
394	0.197	1.00	23.8	(3.6)	46.7	81.0	39	(1.8)
398	0.509	0.401	4.6	7.4	43.6	47.3	5	3.7
404	3.02	2.88	−5.5	−4.2	280.0	276.0	4	−2.1
408	3.98	3.79	−12.9	−10.6	280.5	280.4	2	−5.4
419	1.35	1.25	−0.6	−0.9	271.7	270.1	2	−0.5
423	0.835	0.802	4.7	2.9	57.1	61.0	4	1.5
428	0.932	0.905	4.0	5.6	51.9	52.3	2	2.8
Mean								−1.7 (−2.7)
σ								3.0 (5.0)
$\sigma/N^{1/2}$								0.7 (1.1)
Cores 34–38, N = 9, 312.17 m Below Sea Floor, 35–40 m.y. B.P.								
0	1.89	1.69	−2.6	−3.0	286.5	284.9	2	−1.5
106	1.11	1.04	2.5	2.8	97.4	96.3	1	1.4
941	1.02	1.15	−9.7	−6.4	355.6	351.8	5	−3.2
1044	0.358	0.461	−0.6	0.5	14.7	8.9	6	0.3
1929	1.18		8.2		111.7			4.1*
1964	2.39	2.41	0.4	−0.2	293.3	296.8	4	−0.1
2865	1.17	0.969	5.4	2.5	207.4	207.3	3	1.3
2918	0.956		9.1		61.1			4.6*
3794	0.442		0.0		274.3			0.0*
3897	0.0881		(29.2)		261.0			
Mean								0.8
σ								2.3
$\sigma/N^{1/2}$								0.8
Core 39, N = 20, 359.57 m Below Sea Floor, 41 m.y. B.P.								
0	0.767		−7.6		99.6			−3.8*
11	0.806		0.5		256.9			0.3*
24	0.554		19.0		52.9			9.8*
35	0.825	0.543	17.7	13.2	59.2	65.1	7	6.7
45	0.688	0.413	22.9	20.7	61.6	68.1	6	10.7
68	1.05	0.719	11.9	8.3	158.0	160.4	4	4.2
83	0.675	0.427	17.7	12.5	162.7	168.3	8	6.3
101	1.25	0.801	14.6	9.2	98.2	101.8	6	4.6
117	1.15	0.778	24.5	19.9	94.3	93.6	5	10.3
130	1.26	0.843	11.0	8.4	106.1	100.6	6	4.2
147	0.645	0.361	0.0	−8.2	18.6	19.2	8	−4.1
154	0.478	0.346	1.8	−7.1	30.6	33.1	9	−3.6
169	1.24	0.842	8.2	6.6	290.8	286.0	5	3.3
185	1.13	0.799	12.2	9.6	17.2	21.0	5	4.8
205	1.59	1.14	11.4	14.0	288.6	292.6	5	7.1
211	1.46	1.11	11.1	13.0	292.9	292.9	2	6.6
228	1.05	0.803	15.6	14.6	0.0	3.4	3	7.4
236	0.653	0.481	22.0	20.5	355.9	8.3	12	10.6
258	0.665	0.447	15.4	15.3	327.3	343.2	15	7.8
266	0.732	0.417	8.3	9.0	339.1	346.5	7	4.5
Mean								4.9
σ								4.5
$\sigma/N^{1/2}$								1.0

The depth is the distance from the top of the core. Each sample is approximately 10–20 cm^3. M is magnetization, I is inclination, and D is declination. Subscripts refer to fields of peak ac demagnetization, Δ is a measure of the reliability as defined in the text, and λ_{88} is the paleolatitude after 88-Oe demagnetization. N is the number of samples. Values in parentheses are only included in the means and standard deviations in parentheses.

* NRM value.

precisely the pattern that we hoped might be associated with an equatorial crossing.

A more statistical analysis can be accomplished by determining means and their deviations for each group of samples. So as not to bias our averages we first want to discard any results which either are very different from the others or represent more unstable behavior. We notice that many samples with extreme inclinations also have magnetization directions which change greatly under demagnetization from NRM to 88 Oe, whereas most samples show little change. We quantify this by calculating the angular change between magnetizations at NRM and 88 Oe. This number, Δ, is not a strictly valid criterion of stability, although in general, higher values of Δ correspond to higher values of PSI. We utilize it only as a means of limiting our results so that they all represent similar magnetic behavior. A histogram of Δ values (Figure 6) shows that most are small (<20°), although from Table 1 we can see that samples from different cores show different behavior. Some, like those from core 8, have very low values except for the few that also have extreme values of inclination; others, like those from core 23, have rather high values. In general, we have discarded data from samples with Δ > 25°. In only one case (sample 31-154) have we discarded an extreme inclination that also had low Δ. Mean inclinations of these selected samples are not greatly different from those which include all our samples (Table 1), but standard deviations are in some cases

TABLE 2. Remanent Magnetic Properties for DSDP Sites 290 and 294 Sediments

Depth, cm	M_0, 10^{-4} G cm^3	M_{88}, 10^{-4} G cm^3	I_0, deg	I_{88}, deg	D_0, deg	D_{88}, deg	Δ, deg	λ_{88}, deg
Site 290, Core 2, N = 14, 75.05 m Below Sea Floor, 15 m.y. B.P.								
0	1.70	1.72	−6.8	−7.1	61.5	92.9	31	−3 6
21	0.865	0.643	16.6	−0.2	139.8	106.1	37	−0 1
41	1.31	0.930	−23.4	−25.8	240.6	256.0	14	−13.6
61	1.30	0.832	−5.7	−10.1	253.0	258.0	7	−5.1
81	1.85	1.32	15.2	13.1	240.9	252.5	11	6.6
101	1.10	0.664	1.0	−4.4	237.5	260.4	24	−2.2
121	2.38	1.91	−30.5	−31.9	239.2	252.2	11	−17.3
141	1.23	0.852	−16.9	−23.5	236.3	248.8	13	−12.3
151	0.288	0.370	39.8	28.6	155.2	107.5	41	15.3
174	0.332	0.314	−11.1	(−53.8)	177.5	109.3	68	(−34.3)
191	0.791	0.907	−6.8	−15.2	133.9	101.7	33	−7.7
211	0.688	0.780	−37.8	−34.6	143.2	102.0	33	−19.0
229	1.44	1.26	7.1	8.9	273.3	288.7	15	4.5
251	1.97	1.54	40.0	34.8	256.7	273.6	14	19.2
271	0.745	0.370	−39.9	−40.7	152.6	114.4	29	−23.3
Mean								−4.2 (−5.4)
σ								12.1 (14.1)
$\sigma/N^{1/2}$								3.2 (3.8)
Site 290, Core 7, N = 15, 205.07 m Below Sea Floor, 34–36 m.y. B.P.								
0	0.359	0.523	40.3	37.6	274.4	206.8	51	21.1
15	0.636	0.613	−15.0	−8.9	268.6	248.6	21	−4.5
25	1.25	0.852	3.3	4.6	22.4	41.1	19	2.3
50	3.78	1.31	7.6	8.2	161.3	151.6	10	4.1
98	0.909	1.08	79.3	61.1	260.8	192.3	27	42.2
115	2.23	2.10	21.7	32.4	314.5	317.0	11	17.6
129	2.40	1.92	23.5	34.4	342.1	346.2	12	18.9
156	2.15	1.66	9.1	11.3	6.1	6.4	2	5.7
285	2.71	2.61	60.4	69.2	344.9	343.6	9	52.8
333	3.20	2.87	44.4	51.7	284.8	274.5	10	32.3
353	2.70	2.49	65.3	71.3	292.2	276.1	8	55.9
371	2.92	2.65	61.5	68.0	321.7	302.8	10	51.1
385	2.54	2.57	64.4	63.6	261.3	239.2	10	45.2
408	2.45	2.50	63.9	58.9	119.9	139.8	11	39.7
423	1.80	1.94	20.1	29.2	77.4	102.2	24	15.6
Mean								26.7
σ								19.5
$\sigma/N^{1/2}$								5.0
*Site 294, Core 2, N = 11, 47.39 m Below Sea Floor, 24 m.y. B.P.**								
0	1.34	1.01	60.4	(72.5)	149.2	107.9	20	(57.8)
7	1.59	1.20	45.7	43.0	74.7	73.4	3	25.0
17	0.575	0.202	49.2	46.1	171.6	336.5	84	27.5
26	0.491	0.169	−14.3	(−77.4)	151.4	339.3	88	(−65.9)
35	0.360	0.177	12.3	4.8	213.9	224.7	22	2.4
40	0.717	0.616	−32.6	−39.0	147.7	105.8	34	−22.0
46	0.544	0.643	−21.3	−26.0	108.5	80.1	26	−13.7
57	1.03	0.736	−1.6	−18.2	11.5	2.1	19	−9.3
67	1.11	0.811	14.2	10.8	112.6	95.2	17	5.5
72	0.688	0.450	39.4	53.4	116.5	51.4	45	34.0
85	0.209	0.0762	0.0	15.1	261.5	13.0	111	7.7
93	0.556	0.378	19.6	25.1	168.2	81.7	79	13.2
99	0.443	0.190	10.3	29.0	194.4	301.7	100	15.5
Mean								7.8 (6.0)
σ								16.9 (29.1)
$\sigma/N^{1/2}$								5.1 (8.1)
*Site 294, Core 4, N = 15, 99.05 m Below Sea Floor, 50 m.y. B.P.**								
0	1.58	1.21	2.1	−5.2	301.7	313.5	14	−2.6
5	1.63	1.06	−0.8	1.5	238.5	238.8	2	0.8
11	1.21	0.754	23.3	20.6	169.0	165.4	4	10.6
16	1.77	1.15	58.7	59.7	86.5	77.3	5	40.6
21	1.78	1.41	27.8	21.5	341.9	347.3	8	11.1
26	2.86	1.70	33.6	34.5	186.9	187.7	1	19.0
37	3.12	2.30	9.1	6.6	298.8	305.9	8	3.3
52	4.82	3.29	27.6	30.9	73.6	65.1	8	16.7

TABLE 2. (continued)

Depth, cm	M_0, 10^{-4} G cm^3	M_{88}, 10^{-4} G cm^3	I_0, deg	I_{88}, deg	D_0, deg	D_{88}, deg	Δ, deg	λ_{88}, deg
*Site 294, Core 4, N = 15, 99.05 m Below Sea Floor, 50 m.y. B.P.** (continued)								
58	2.05	1.72	22.2	19.4	349.3	350.6	3	10.0
68	1.28	0.897	−2.6	−3.3	222.6	330.6	8	−1.7
78	2.39	1.66	56.2	51.8	70.4	58.7	8	32.4
88	0.733	0.475	2.0	−5.7	192.8	202.4	12	−2.9
98	0.328	0.200	47.3	48.5	128.7	80.0	32	29.5
108	0.366	0.0815	21.5	24.2	190.3	185.0	6	12.7
118	0.442	0.149	58.5	32.8	276.2	336.8	47	17.9
Mean								13.2
σ								12.8
$\sigma/N^{1/2}$								3.3

The depth is the distance from the top of the core. Each sample is approximately 10–20 cm^3. M is magnetization, I is inclination, and D is declination. Subscripts refer to fields of peak ac demagnetization; Δ is a measure of the reliability as defined in the text, and λ_{88} is the paleolatitude after 88-Oe demagnetization. N is the number of samples. Values in parentheses are only included in the means and standard deviations in parentheses.

*A sedimentation rate of 2.0 m/m.y. is assumed.

greatly reduced. In all but one case we use the actual sign of the inclinations and assume that the values in each group are not affected by reversals of the earth's field. By so doing we produce distribution patterns (Figure 5) more similar to Gaussian than they would be if we took absolute values and assumed that all changes in sign were caused by reversals. The only exception to this is in core 18, where a sequence of three positive inclinations shifts abruptly to negative values. This we attribute to a reversal.

Mean paleolatitudes and their 95% confidence intervals are plotted in Figure 7 as a function of age. Here we can clearly see the northward motion and equatorial crossing of site 292. The sign of the paleolatitude is uniquely determined by considering the trend as a function of age. Only if rather discontinuous plate motions occurred could the northern latitude location for core 39 be possible. A mean paleolatitude for 35 basalt samples agrees with these basal sediments, although its standard error is large because of incomplete sampling of secular variations. The ability of the sediments to average out secular variations in paleopole positions allows them a far greater precision; in the best cases they have a 95% confidence interval of less than 5°.

Of course, when we calculate paleolatitudes from our paleoinclinations, we use the equation for a geocentric dipole,

$$\tan I = 2 \tan \phi \qquad (1)$$

where I is the inclination and ϕ is the latitude. If the dipole is not geocentric but has been shifted northward in the past, as is suggested by several authors [*Wilson*, 1970; *Wilson and McElhinny*, 1974], then that shift would produce an apparent northward motion for a fixed site when the paleomagnetic data from that site are analyzed with the geocentric equation. We should really use the equation for an offset dipole,

$$\tan I = \frac{2 \cos \theta + 2r^2 \cos \theta - r \cos^2 \theta - 3r}{\sin \theta (1 + r \cos \theta - 2r^2)} \qquad (2)$$

where θ is the colatitude of our site and r is the northward offset in the dipole expressed as a fraction of the earth's radius. However, to produce a large enough effect for θ fixed at 75° to fit Figure 7 by increasing r, we would need a maximum offset larger than 1000 km. This is several times as large as values which have recently been suggested [*Wilson and McElhinny*, 1974]. Also our purpose is to compare our paleomagnetic results with those from magnetic anomalies. Northward shifts in the dipole would affect both results and would not interfere with such a comparison.

Sites 290 and 294

The one major assumption that we do make in order to compare our site 292 paleomagnetic results directly with those from the phase shifting of magnetic anomalies is that they are both part of the same rigid plate. They do lie near each other, but this still does not make this assumption entirely obvious. Site 292 is situated on an anomalous and poorly understood feature, the Benham Rise, while the magnetic anomalies are all located in the deepwater regions of the basin. We must therefore show that our paleomagnetic analysis of site 292 is not unique to it but is also valid for other sites in the West Philippine Basin.

Sites 290 and 294 (Figure 1) offer the only other relatively undisturbed sedimentary sections in the West Philippine Basin, but these do not consist of as promising a material as does site 292. Only a few cores were recovered at each site, sedimentation rates are low (0.2–0.3 cm/10^3 yr), and the sediment contains few microfossils. The lithologies are variable and quite different from those of site 292. Site 290 consists of a zeolite-rich clay/ash in core 2 and a nannofossil-rich volcanic ash in core 7; site 294 contains a brown clay in core 2 and a clay with palagonite ash in core 4. Most of these differences are due primarily to the greater water depths (6063 m at site 290 and 5784 m at site 294), which place the sedimentary regime well below the CCD [*Ingle et al.*, 1975].

We collected a total of 58 samples from two cores in each of sites 290 and 294. A pilot study of eight of these shows (Figure 8) that they are less stable than are the site 292 samples and that 175 Oe may have been a better choice for a standard field of demagnetization than the 88 Oe which was our value for all nonpilot samples. Values for Δ (Table 2) are higher than those for site 292 and show a different distribution in the histogram of Figure 6. It is therefore not surprising that we find the standard deviations of mean paleolatitudes from these sites to be much larger than those for site 292.

Figure 9 shows mean paleolatitudes for sites 290 and 294 as a function of time. The paleolatitudes themselves are not very definitive owing to their large intervals of 95% confidence, but we can still use them as a test for values predicted by the

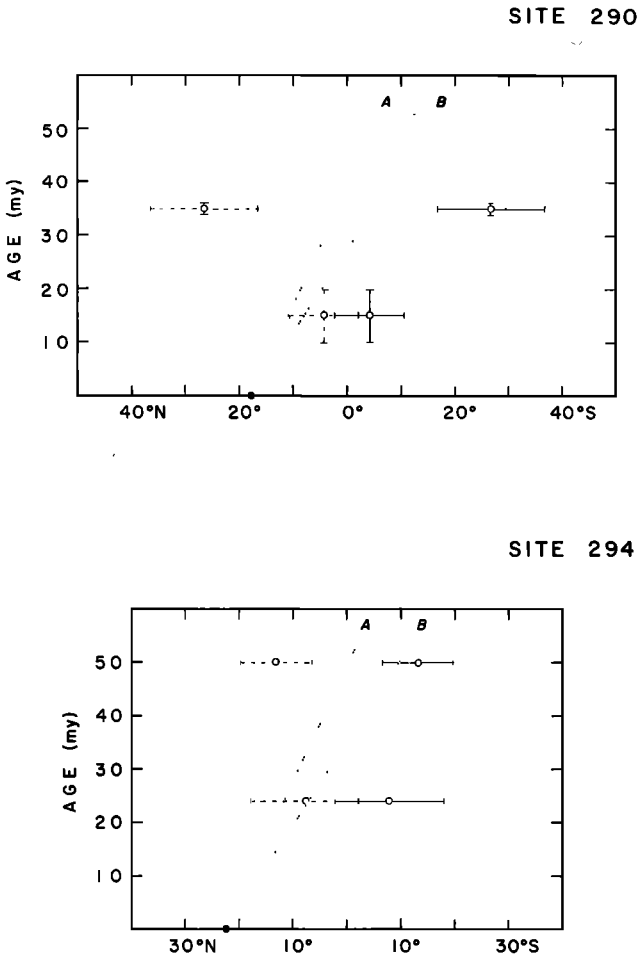

Fig. 9. Paleolatitudes versus age for sites 290 and 294. Means and ±2 standard errors are plotted for two groups of samples at each site. Ages for site 294 are based on an assumed sedimentation rate of 2.0 m/m.y. For site 290 they are based on nannofossil assemblages [*Ellis*, 1975] and the *Berggren* [1972] time scale. Values on either side of the equator are equally possible, and both are plotted for each determination. With the exception of the oldest paleolatitude for site 290, origins south of the equator are consistent with lines A and B defined in Figure 7 for the motion of site 292. This agreement suggests that paleolatitude determinations for site 292 are not governed by the possibly anomalous tectonic setting of the Benham Rise (site 292).

motion of site 292. These predictions are based on the two lines A and B, which are determined in Figure 7. Line A is a visual best fit that is constrained to go through the present latitude of site 292, while line B fits only the five oldest paleolatitudes. These same lines, plotted in Figure 9 to go through the present latitudes of sites 290 and 294, also fit the older paleolatitude measurements. The one exception is the oldest paleolatitude determination for site 290, which is located at a higher latitude than its prediction.

Paleopoles and Relative Rotations

Paleopoles can be determined from the shape of sea floor spreading magnetic anomalies [*R. L. Larson and C. G. Chase*, 1972; *Schouten and Cande*, 1976; *Louden*, 1976]. The technique is to describe the anomaly in the wave number domain:

$$M(k) = C \cdot J(k) \cdot E(k) \cdot e^{-i\theta} \quad (3)$$

where $M(k)$ is the Fourier transform of the magnetic anomaly $m(x)$, C is a constant, $J(k)$ is the transform of the magnetization distribution $j(x)$, and $E(k)$ is the magnetic earth filter [*Schouten and McCamy*, 1972]. The effect of phase filter $e^{-i\theta}$ can be removed by multiplying $M(k)$ by $e^{i\theta}$ for the appropriate value of θ, and a 'deskewed' (i.e., square wave looking) pattern should result. This θ gives the set of all possible remanent inclinations and declinations, which map as a great circle on a stereonet plot of paleonorth poles [*Schouten and Cande*, 1976].

We apply this technique on a short sequence of anomalies in the West Philippine Basin first described by *Louden* [1976]. Figure 10 gives the location and identification of these anomalies. These identifications are consistent with the paleontological dates from DSDP site 291 [*Ingle et al.*, 1975] and an origin south of the equator, which is supported by the paleomagnetic measurements described in this paper. The phase-shifted anomalies and degree of phase shift are shown in Figure 11. These values are little changed from the previous estimates of *Louden* [1976] and range from 160° to 200° for the various profiles. This range of θ is plotted as a range of paleopole positions in Figure 12*a* and is consistent with the sediment paleolatitudes for DSDP sites 292, 294, and 290, which plot as small circles of paleopole positions in Figure 12*b*.

Watts et al. [1977] have suggested that there is a skewness shift of 30°–70° in anomalies on opposing sides of the Central Basin Fault (Figure 1). *Cande* [1976] reports similar although somewhat smaller differences in anomalies 27–32 across the Pacific-Antarctic ridge. He suggests that these differences might be due to tectonic effects and that the true θ value should be the average of the values on either side of the ridge. If this is true for anomalies across the Central Basin Fault, we should use a somewhat larger value (200°–220°) for θ, since the anomalies treated in this paper all lie to the south of it. This will not be a serious complication in our subsequent analysis because (1) the value of θ is not the primary factor in delimiting a paleopole position and (2) the agreement between paleomagnetic and phase-shifting inclinations suggests that the skewness of the anomalies is a true indicator of the remanent magnetic field.

The one remaining parameter which also depends on the remanent inclination and declination is the amplitude factor C in (3),

$$C = (\sin I \sin I_r)/(\sin I' \sin I_r') \quad (4)$$

where $\tan I_r' = \tan I_r / \sin \alpha_r$. For the anomalies of Figures 10 and 11, C can range from 0 to 0.94, depending on the value of the remanent strike α_r. Values of C along $\theta = 180°$ are plotted in Figure 12*a*.

The range of possible pole positions will be greatly restricted if we can place limits on this parameter. To do this, we must assume that the magnetic source layer thickness and magnetization are similar to those that form anomalies in other ocean basins where C is known. There are as yet few data on which to base this assumption. The only large quantity of basalts collected by DSDP in the West Philippine Basin is from site 292 (Figure 1). We studied 34 samples of this basalt and found a mean susceptibility and standard deviation of $1.28 \pm 0.25 \times 10^{-3}$ G/Oe and a Königsberger ratio of 5.26 ± 3.99. These are within the range of results from the North Pacific [*Lowrie et al.*, 1973*a*] and Atlantic [*Lowrie et al.*, 1973*b*] oceans. However, the thickness of the magnetic source layer is not known. There is some recent evidence that the crust in the Philippine Sea as determined by seismic refraction is 1–2 km thinner than that in the Pacific [*Sclater et al.*, 1976], but the implication that this might have on the magnetic properties of the upper crust is uncertain.

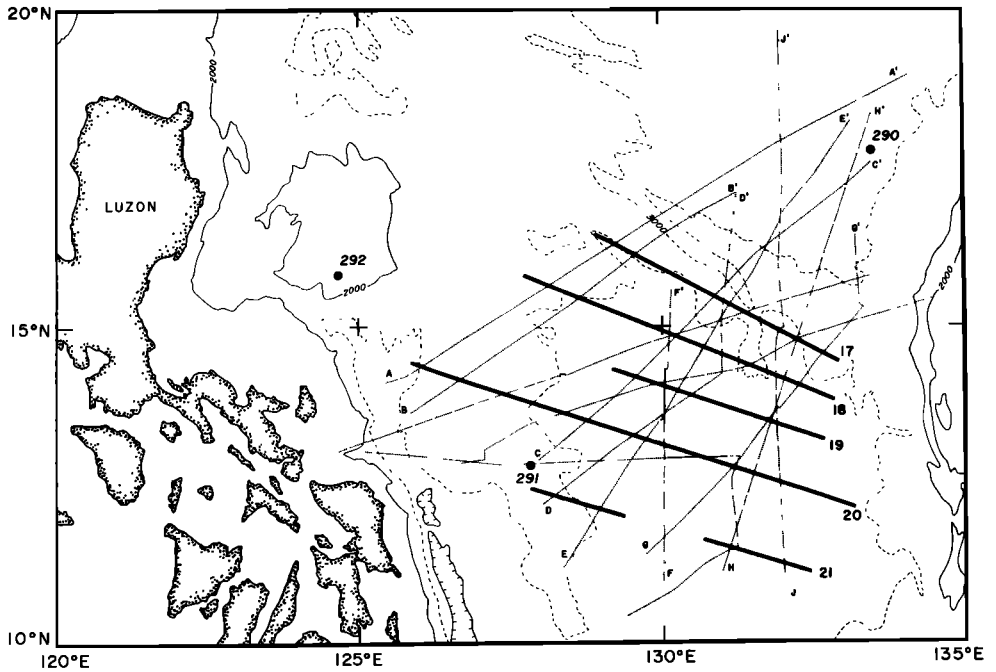

Fig. 10. Map of DSDP sites, ship tracks, and magnetic anomalies in the West Philippine Basin (see Figure 1 for location). Alphabetic labels identify ship track segments used in Figure 11. Numbers identify anomalies as reported by *Heirtzler et al.* [1968].

In the absence of any conflicting data we will assume that the origins of our anomalies are the same as those for anomalies in other ocean basins. We can determine C by comparing the amplitude of our anomalies to those where C is known. This is done in Table 3, where we list all of the major east-west anomalies. All amplitudes of east-west anomalies with C close to unity are large (700–1000 γ), a result which implies that our small-amplitude (200–300 γ) anomalies in the West Philippine Basin must have a smaller value for their amplitude factor. This is possible only if this plate underwent significant rotation in the past. Taking $0.2 \leq C \leq 0.6$ limits our locus of pole positions in Figure 12*a* to two areas at either extreme of our great circles, both of which are consistent with mean paleolatitudes for DSDP sites 292 and 294 (Figure 12*c*).

We can compare our West Philippine Basin paleomagnetic pole positions to predictions based on known plate rotations. The rotation of the Philippine plate with respect to the spin axis is the vector sum of rotations of the Pacific plate relative to the spin axis and of the Philippine plate with respect to the Pacific:

$$_{\text{Phil}}\omega_{\text{pole}} = {}_{\text{Phil}}\omega_{\text{Pac}} + {}_{\text{Pac}}\omega_{\text{pole}} \qquad (5)$$

Finite rotations of the Pacific with respect to the pole are recorded in bathymetric lineations such as the Emperor-Hawaiian seamount chain. Various determinations of this pole have been made (see *Solomon and Sleep* [1974] for a summary), but differences are not significant in this study. We use the *Minster et al.* [1974] pole (67°S, 121°E) and rate (8×10^{-7} deg/yr) over the past 40 m.y. Since our anomalies are as old as 50 m.y., we add to this a rotation of 10° (10^{-6} deg/yr over 10 m.y.) about the *Clague and Jarrard* [1973] pole (17°S, 73°E) determined from the Emperor seamount chain.

The only information concerning $_{\text{Phil}}\omega_{\text{Pac}}$ comes from fitting fault plane solutions for recent earthquakes on the margins of the Philippine plate. This has been done by *Katsumata and*

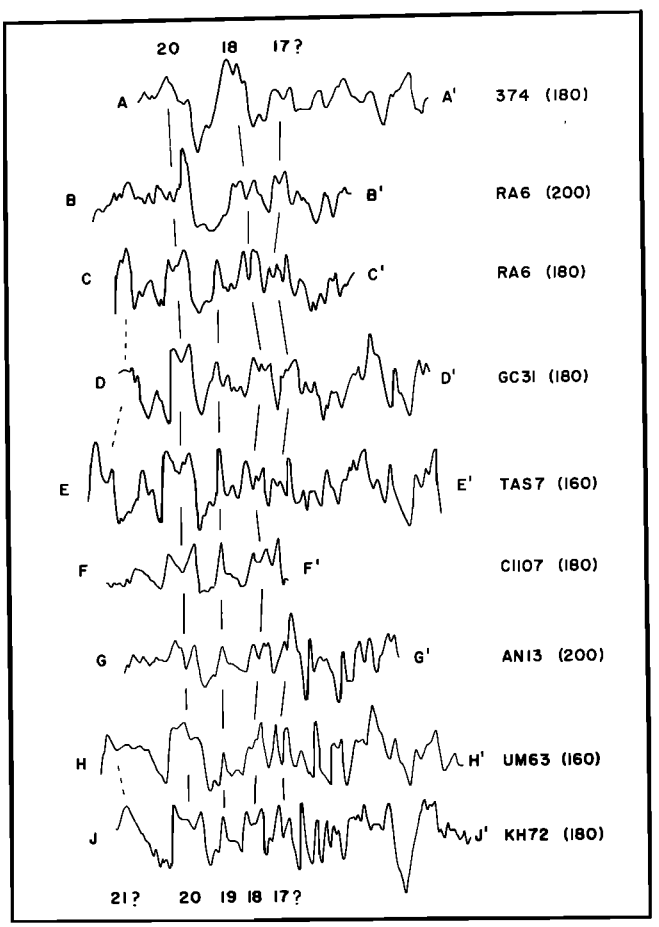

Fig. 11. Phase-shifted anomalies from tracks in Figure 10 projected along N21°E. Degree of phase shift is given in parentheses next to the cruise identification for each track. Correlation of anomalies is extended from the original identification of *Louden* [1976].

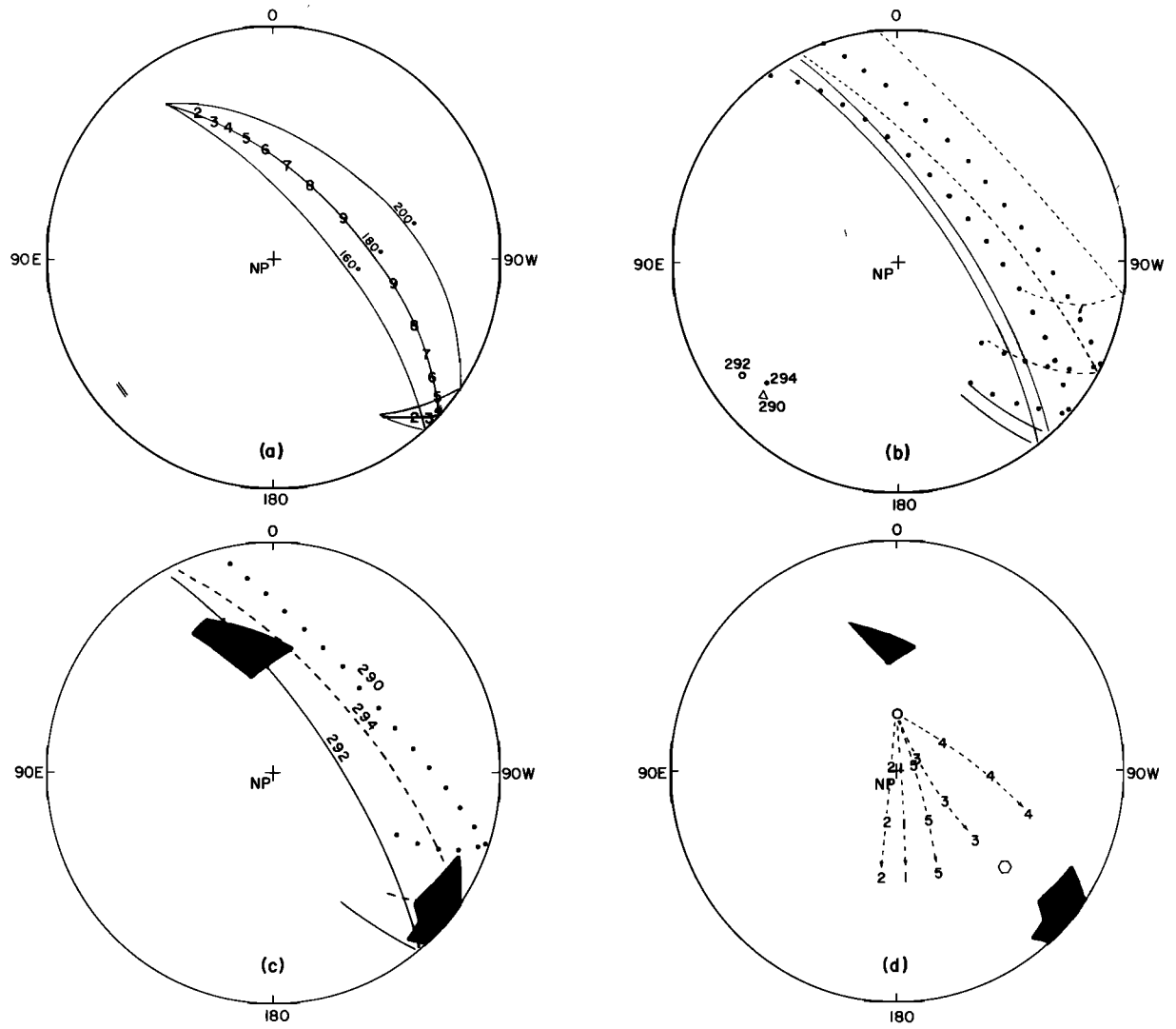

Fig. 12. Stereonet projections of paleomagnetic pole positions. (*a*) Great circles determined from the phase shifting of magnetic anomalies (Figure 11). Individual circles correspond to phase shifts of 160°, 180°, and 200°. Numbers correspond to magnetic anomaly amplitude factors of 10*C* as defined in the text. (*b*) Small circles determined from paleolatitude measurements on sediments of DSDP sites 290 (dashed lines), 292 (solid lines), and 294 (dotted lines). Pairs of lines enclose areas of 95% confidence. (*c*) Combined plots of mean paleolatitude data (lines) and phase shifting (shaded regions) where $0.2 \leq C \leq 0.6$. The amplitude constraint is determined from comparison with other east-west anomalies (Table 3). (*d*) Shaded regions include the region of Figure 12*c* which falls between site 292 and 294 paleomagnetic data. The hexagon is the mean pole position for Guam Miocene volcanics [*E. E. Larson et al.*, 1975]. Numbers indicate paleopole determinations from the motion of the Pacific-Philippine plate for various relative Phil-Pac poles: 1 is at −5°, −52° from *Karig* [1975]; 2 at −3°, −63° from *Karig* [1975]; 3 at 26°, −37° from *Fitch* [1972]; 4 at −1°, 1° from *Fitch* [1972]; and 5 at −7°, −38° from *Katsumata and Sykes* [1969]. Each successive number represents an additional 20° of relative Phil-Pac rotation away from the Pacific paleopole for 50 m y. B.P. (open circle), which is calculated from motions of *Minster et al.* [1974] and *Clague and Jarrard* [1973].

Sykes [1969] for earthquakes on the Izu-Bonin margin of the Pacific and Philippine plates and by *Fitch* [1972] and *Karig* [1975] for earthquakes on the Japan-Ryukyu margin of the Philippine and Eurasia plates. These solutions are then summed with Eurasia-Pacific rotations to determine a Philippine-Pacific pole. These pole positions are not well constrained, are poorly located, and of course are only instantaneous and need not apply over a finite time period. We use them only as a point of reference.

Figure 12*d* shows the results of calculations based on (5). Paleomagnetic pole positions are calculated for varying amounts of rotation about the different Pacific-Philippine poles. Only one of our two possible pole positions is compatible with these rotations. Plate motion between the Philippine and the Pacific plate would have to have been the reverse of what it is today for the other paleopole to be possible. This is evidence for a large amount (60°) of clockwise rotation between the Pacific and the Philippine plate, which conforms to the theory of *Uyeda and Ben-Avraham* [1972].

The paleopole position for Miocene volcanic rocks on Guam [*E. E. Larson et al.*, 1975] also records a large clockwise rotation (Figure 12*d*). These rocks date from the Miocene pulse of volcanism, which *Karig* [1975] believes is coincident with the opening of the Parece Vela Basin. A hypothetical polar wandering curve can simultaneously explain these rotations and the rotations of the West Philippine Basin, in which

TABLE 3. Magnitude and Location of Major East-West Sea Floor Spreading Magnetic Anomalies

Identification	Anomaly	Site Latitude	Site Longitude	Paleopole Latitude	Paleopole Longitude	Peak to Peak Magnitude	C^*	Reference
Phoenix	M1–M10	5°N	175°W	50°N	30°W	1000	0.84	*R. L. Larson and C. G. Chase* [1972]
Wharton Basin†	21	20°S	84°E	71°S	126°E	700	1.0	*Sclater and Fisher* [1974]
North Pacific	27–32	50°N	170°W	68°N	20°E	1000	1.0	*Cande* [1976]
Galápagos	3–5	3°N	87°W	90°N		700	1.0	*Sclater and Klitgord* [1973]
Philippine Sea	20	15°N	130°E	3°N	130°E	200–300	0.40	this paper

*C = (sin I sin I_r)/(sin I' sin I_r'), where I is the inclination, I' is the effective inclination, and r refers to remanent values.
†The paleopole position is assumed to be the same as that for Australia.

case the motion of Guam would not be caused by a simple bending of the Marianas island arc as *E. E. Larson et al.* [1975] suggest. Interarc spreading between Guam and the West Philippine Basin might not have disrupted the major clockwise rotation of the Philippine plate with respect to the Pacific over the past 50 m.y.

CONCLUSIONS

The following list is a summary of the major results of this study:

1. Sediment cores taken by the DSDP can yield well-grouped paleolatitudes, especially when results of closely spaced samples can be averaged together at several separate locations downcore. These results can be of greater resolution than those from DSDP basalts, which may not contain enough flow units to average out components of secular variation adequately.

2. Paleolatitudes for DSDP site 292 sediments indicate that this site formed south of the equator, and results for sites 290 and 294 can be explained in a similar manner. This adds independent justification for our inversion of magnetic anomalies in the West Philippine Basin with respect to North Pacific anomalies, which is necessary in order to identify them with worldwide Eocene reversals.

3. Paleomagnetic pole positions determined from both the phase shifting of magnetic anomalies and the paleomagnetics of DSDP sites in the West Philippine Basin are consistent with each other and can be restricted to two relatively well defined positions if the low amplitude of the anomalies is due to a rotation of the Philippine plate. One of these two positions, which includes a large amount of clockwise rotation of the Philippine plate with respect to the magnetic pole, is consistent with the finite absolute rotations of the Pacific plate and present Philippine-Pacific plate rotations. It is also consistent with paleopole positions for Guam and may mean that both have undergone the same motions since the early Miocene.

Acknowledgments. This research was supported by Office of Naval Research contract N00014-75-C-0219. I would like to thank John Sclater for his support of this work, C. E. Helsley for offering the use of his paleomagnetics facilities at the University of Texas at Dallas, and Charles Denham for valuable contributions at all stages of this project. Hans Schouten first suggested using the amplitude factor to help constrain the paleomagnetic pole position. Charles Denham and Hans Schouten made valuable criticisms of an earlier version of this paper. Woods Hole Oceanographic Institution contribution 3538.

REFERENCES

Berggren, W. A., A Cenozoic time-scale—Some implications for regional geology and paleobiogeography, *Lethaia, 5*, 195–215, 1972.

Blow, R. A., and N. Hamilton, Paleomagnetic evidence from DSDP cores of northward drift of India, *Nature, 257*, 570–572, 1975.

Cande, S., Paleomagnetic poles from Late Cretaceous marine magnetic anomalies in the Pacific, *Geophys. J. Roy. Astron. Soc., 44*, 547–566, 1976.

Chase, T. E., and H. W. Menard, Bathymetric atlas of the northwest Pacific Ocean, Inst. of Mar. Resour., Scripps Inst. of Oceanogr., Univ. of Calif., San Diego, 1969.

Clague, D. A., and R. D. Jarrard, Tertiary Pacific plate motion deduced from the Hawaiian-Emperor chain, *Geol. Soc. Amer. Bull., 84*, 1135–1154, 1973.

Creer, K. M., R. Thompson, L. Molyneux, and F. J. H. Mackereth, Geomagnetic secular variation recorded in the stable magnetic remanence of recent sediments, *Earth Planet. Sci. Lett., 14*, 115–127, 1972.

Ellis, C. H., Calcareous nannofossil biostratigraphy, Leg 31, in *Initial Reports of the Deep-Sea Drilling Project*, vol. 31, edited by J. C. Ingle et al., pp. 655–676, U.S. Government Printing Office, Washington, D. C., 1975.

Fitch, T. J., Plate convergence, transcurrent faults, and internal deformation adjacent to southeast Asia and the western Pacific, *J. Geophys. Res., 77*, 4432–4460, 1972.

Francheteau, J., C. G. A. Harrison, J. G. Sclater, and M. L. Richards, Magnetization of Pacific seamounts: A preliminary polar curve for the northeastern Pacific, *J. Geophys. Res., 75*, 2035–2061, 1970.

Green, K. E., and A. Brecher, Preliminary paleomagnetic results for sediments from site 263, Leg 27, in *Initial Reports of the Deep-Sea Drilling Project*, vol. 27, edited by J. J. Veevers et al., pp. 405–413, U.S. Government Printing Office, Washington, D. C., 1974.

Hammond, S. R., F. Theyer, and G. H. Sutton, Paleomagnetic evidence of northward movement of the Pacific plate in deep-sea cores from the central Pacific basin, *Earth Planet. Sci. Lett., 22*, 22–28, 1974.

Hammond, S. R., L. W. Kroenke, F. Theyer, and D. L. Keeling, Late Cretaceous and Paleogene paleolatitudes of the Ontong Java Plateau, *Nature, 255*, 46–47, 1975.

Harrison, C. G. A., The paleomagnetic record from deep-sea sediment cores, *Earth Sci. Rev., 10*, 1–36, 1974.

Harrison, C. G. A., R. D. Jarrard, V. Vacquier, and R. L. Larson, Paleomagnetism of Cretaceous Pacific seamounts, *Geophys. J. Roy. Astron. Soc., 42*, 859–882, 1975.

Heirtzler, J. R., G. O. Dickson, E. M. Herron, W. C. Pitman III, and X. Le Pichon, Marine magnetic anomalies, geomagnetic field reversals, and motions of the ocean floor and continents, *J. Geophys. Res., 73*, 2119–2136, 1968.

Ingle, J. C., D. E. Karig, H. H. Bouma, C. H. Ellis, N. Haile, I. Koizumi, H. Y. Ling, I. MacGregor, C. Moore, H. Ujiie, T. Watanabe, S. M. White, and M. Yasui, *Initial Reports of the Deep-Sea Drilling Project*, vol. 31, U.S. Government Printing Office, Washington, D. C., 1975.

Karig, D. E., Basin genesis in the Philippine Sea, in *Initial Reports of the Deep-Sea Drilling Project*, vol. 31, edited by J. C. Ingle et al., pp. 857–879, U.S. Government Printing Office, Washington, D. C., 1975.

Katsumata, M., and L. R. Sykes, Seismicity and tectonics of the western Pacific: Izu-Mariana, Caroline, and Ryukyu-Taiwan regions, *J. Geophys. Res., 74*, 5923–5948, 1969.

Larson, E. E., R. L. Reynolds, M. Ozima, Y. Aoki, H. Kinoshita, S. Zasshu, N. Kawai, T. Nakajima, K. Hirooka, R. Merrill, and S. Levi, Paleomagnetism of Miocene volcanic rocks of Guam and the

curvature of the southern Mariana island arc, *Geol. Soc. Amer. Bull., 86,* 346–350, 1975.
Larson, R. L., and C. G. Chase, Late Mesozoic evolution of the western Pacific Ocean, *Geol. Soc. Amer. Bull., 83,* 3627–3644, 1972.
Louden, K. E., Magnetic anomalies in the West Philippine Basin, in *The Geophysics of the Pacific Ocean Basin and Its Margin, Geophys. Monogr. Ser.,* vol. 19, edited by G. H. Sutton, M. H. Manghnani, and R. Moberly, pp. 253–267, AGU, Washington, D. C., 1976.
Lowrie, W., R. Løvlie, and N. D. Opdyke, Magnetic properties of Deep-Sea Drilling Project basalts from the North Pacific Ocean, *J. Geophys. Res., 78,* 7647–7660, 1973*a*.
Lowrie, W., R. Løvlie, and N. D. Opdyke, The magnetic properties of Deep-Sea Drilling Project basalts from the Atlantic Ocean, *Earth Planet. Sci. Lett., 17,* 338–349, 1973*b*.
McKenzie, D. P., and J. G. Sclater, The evolution of the Indian Ocean since the Late Cretaceous, *Geophys. J. Roy. Astron. Soc., 25,* 437–528, 1971.
Minster, J. B., T. H. Jordan, P. Molnar, and E. Haines, Numerical modeling of instantaneous plate tectonics, *Geophys. J. Roy. Astron. Soc., 36,* 541–576, 1974.
Opdyke, N. D., Paleomagnetism of deep sea cores, *Rev. Geophys. Space Phys., 10,* 213–249, 1972.
Peirce, J. W., Assessing the reliability of DSDP paleolatitudes, *J. Geophys. Res., 81,* 4173–4187, 1976.
Phillips, J. D., and D. Forsyth, Plate tectonics, paleomagnetism, and the opening of the Atlantic, *Geol. Soc. Amer. Bull., 83,* 1579–1600, 1972.
Schouten, H., and S. C. Cande, Paleomagnetic poles from sea-floor spreading anomalies, *Geophys. J. Roy. Astron. Soc., 44,* 567–575, 1976.
Schouten, H., and K. McCamy, Filtering marine magnetic anomalies, *J. Geophys. Res., 77,* 7089–7099, 1972.
Sclater, J. G., and A. Cox, Paleolatitudes from Joides deep sea sediment cores, *Nature, 226,* 934–935, 1970.
Sclater, J. G., and R. L. Fisher, Evolution of the east central Indian Ocean, with emphasis on the tectonic setting of the Ninetyeast Ridge, *Geol. Soc. Amer. Bull., 85,* 683–702, 1974.
Sclater, J. G., and K. D. Klitgord, A detailed heat flow, topographic, and magnetic survey across the Galápagos spreading center, *J. Geophys. Res., 78,* 6951–6975, 1973.
Sclater, J. G., R. N. Anderson, and M. L. Bell, Elevation of ridges and evolution of the central eastern Pacific, *J. Geophys. Res., 76,* 7888–7915, 1971.
Sclater, J. G., D. Karig, L. A. Lawver, and K. Louden, Heat flow, depth, and crustal thickness of the marginal basins of the south Philippine Sea, *J. Geophys. Res., 81,* 309–318, 1976.
Solomon, S. C., and N. H. Sleep, Some simple physical models for absolute plate motions, *J. Geophys. Res., 79,* 2557–2567, 1974.
Symons, D. T. A., and M. Stupavsky, A rational paleomagnetic stability index, *J. Geophys. Res., 79,* 1718–1720, 1974.
Uyeda, S., and Z. Ben-Avraham, Origin and development of the Philippine Sea, *Nature London Phys. Sci., 240,* 176–178, 1972.
Watts, A. B., J. K. Weissel, and R. L. Larson, Sea floor spreading in marginal basins of the western Pacific, *Tectonophysics, 37,* 167–181, 1977.
Wilson, R. L., Permanent aspects of the earth's non-dipole magnetic field over upper Tertiary times, *Geophys. J. Roy. Astron. Soc., 19,* 417–437, 1970.
Wilson, R. L., and M. W. McElhinny, Investigations of the large scale paleomagnetic field over the past 25 million years, Eastward shift of the Icelandic spreading ridge, *Geophys. J. Roy. Astron. Soc., 39,* 570–586, 1974.

(Received June 9, 1976;
revised December 27, 1976;
accepted February 28, 1977.)